



1 **Resolving uncertainties in the application of zircon Th/U and**
2 **CL gauges to interpret U-Pb ages: a case study of eclogites in**
3 **polymetamorphic terranes of NW Iberia**

4

5 Pedro Castiñeiras¹, Juan Gómez Barreiro², Francisco J. Fernández³, Carmen Aguilar⁴
6 and José Manuel Benítez Pérez⁵

7

8 ¹Departamento de Petrología y Geoquímica, Universidad Complutense de Madrid, José Antonio Novais 12,
9 28040 Madrid (Spain).

10 ²Departamento de Geología. Universidad de Salamanca. Facultad de Ciencias, Pza. de los Caídos s/n, 37008
11 Salamanca (Spain).

12 ³Departamento de Geología., Universidad de Oviedo, Jesús Arias de Velasco s/n, 33005 Oviedo (Spain).

13 ⁴Centre for Lithospheric Research, Czech Geological Survey, Klárov 3, 11821 Prague, Czech Republic.

14 ⁵Centro de Ciências e Tecnologias Nucleares. Instituto Superior Técnico. Universidad de Lisboa. Estrada
15 Nacional 10 (km 139,7), 2695-066, Bobadela LRS, Portugal

16 *Correspondence to:* J. Gómez Barreiro (jusb@usal.es)

17

18 castigar@ucm.es
19 brojos@geol.uniovi.es
20 carmen.gil@geology.cz
21 jose.benitez@ctn.tecnico.ulisboa.pt

22

23 **Abstract.** Zircon crystal texture and Th/U ratio have been used as a watertight argument when interpreting U-
24 Pb ages. The wide, and sometimes indiscriminate, use of those gauges could result into  interpretation of the
25 geological meaning of U-Pb data. A case study is presented here where  zircons from a  controversial  polymetamorphic  eclogite unit were analyzed with SHRIMP.  U-Pb and trace element (TE) data were
26 collected for each  point. The combination  of TE and  structural arguments indicates that zircon was part of the
27 eclogite facies mineral assemblage at  390 Ma. However, using Th/U ratio and CL textures lead to  a different  interpretation. Our results suggest that in complex orogenic scenarios and extreme environments well-known
28 techniques (CL) and geochemical relationships (Th/U) must be used in combination with TE data and structural
29 relationships as provenance/process gauges.  While geochronology provides accurate isotope relationships, their
30 temporal dimension must rely on  structural and petrological evidence.

31

32

33

34 **1 Introduction**



35 Dating metamorphic rocks using the U-Pb isotopic system in zircon can be a challenging task owing to
36 the ability of this mineral to grow in a variety of geological conditions and its relative resistance to metamorphic
37 processes. When the evolution of a rock results in complex textures in zircon, the combination of the high
38 spatial resolution provided by the SIMS (secondary ionization mass spectrometry) instruments together with
39 cathodoluminescence (CL) or backscattered (BS) images has turned out to be very convenient in most cases to
40 decipher this intricate history (see Corfu et al., 2003). As most of the geological processes result in a specific set
41 of zircon textures under CL or BS, this methodology strongly relies in our ability to recognize the origin of
42 zircon based on those textures, so we can link the obtained ages to specific geological processes. For example,
43 the most frequent texture in metamorphic zircon is homogeneous zoning found in discordant rims (Rubatto and
44 Gebauer, 2000), patchy zoning is commonly found in eclogitic zircon (Tomaschek et al., 2003), soccer-ball
45 zoning appears in high-grade metamorphic rocks (Fernández Suárez et al., 2007), surrounded and truncated
46 internal areas are considered inherited zircon (xenocrystic cores), and oscillatory zoning is typical of magmatic
47 zircon (Corfu et al., 2003). However, there is a lack of understanding of the zircon growth process, precluding in
48 some cases a straightforward distinction between magmatic and metamorphic zircon (e.g., Harley and Black,
49 1997; Corfu et al., 2003; Kelly and Harley, 2005). Furthermore, experimental data are scarce and technically
50 challenging (e.g., Ayers et al., 2003), limiting our interpretation of growth ages. This is particularly true when
51 high pressure and high temperature conditions are explored, or when we are dealing with suspected
52 polymetamorphic terranes. Metamorphic growth of zircon may occur not only during the thermal peak, but also
53 along the prograde and retrograde path (Roberts and Finger, 1997; Liati and Gebauer, 1999; Vavra et al., 1999;
54 Hermann et al., 2001). Moreover, it is commonly accepted that Th/U ratios lower than 0.1 indicate zircon
55 growth under metamorphic conditions, whereas higher ratios are found in magmatic environments (Williams et
56 al., 1997).

57

58 However, some of these one-to-one correspondences have been defied in a few cases; whether it be
59 metamorphic zircon with high Th/U ratios (see Harley et al., 2007 and references therein) or the unconventional
60 correspondence between oscillatory zoning and an eclogitic origin for zircon (Gebauer et al., 1997; Rubatto et
61 al., 1998; Bingen et al., 2001; Corfu et al., 2002; cited by Corfu et al., 2003). In such cases, the problem is
62 solved falling back on previous geochronological studies to interpret the obtained age, but the distinctive
63 composition of zircon grown under eclogitic conditions can be used as well to determine its origin (e.g. Young
64 and Kylander-Clark, 2015; Paquette et al., 2017; Lotout et al., 2018).

65

66 In this paper, we present one of these examples where both the zircon texture and the Th/U ratio
67 strongly suggest that the obtained age could be interpreted as igneous; whereas, in addition to regional evidence,
68 the REE composition of zircon provides a more complete way to link ages to geological processes.

69 2 Geological Setting

70

71 The Cabo Ortegal Complex is one of the allochthonous complexes cropping out in NW Iberia. These
72 complexes record the protracted history of the northern margin of Gondwana from Cambrian-Ordovician times
73 to the Variscan orogeny (Martínez Catalán et al., 2009, 2019). A recent paper explores the connection between



73 the Iberian allochthonous complexes and some units present in the Armorican Massif (Ballèvre et al., 2014),
74 grouping all of them into lower, middle and upper allochthon depending on their tectonometamorphic evolution
75 and structural position. In NW Iberia, the lower allochthon is a Lower Cambrian siliciclastic sequence, intruded
76 by a Lower Ordovician bimodal magmatism, which experienced high pressure and low to intermediate
77 temperature metamorphism during the Middle Devonian (Díez Fernández et al., 2012a, 2012b; Abati et al.,
78 2010; López Carmona et al., 2013). It represents the most external margin of Gondwana. The middle allochthon
79 is mainly composed of mafic and ultramafic rocks interpreted as fragments of oceanic lithosphere; the oldest
80 (~495 Ma) is related to the Iapetus-Tornquist Ocean, whereas the youngest (~395 Ma) is probably related to the
81 Rheic Ocean (see Arenas et al., 2014, Martínez Catalán et al., 2019 and references therein). The upper
82 allochthon is interpreted as a volcanic arc, and it can be divided according to their metamorphic evolution into
83 HP-HT units, bellow, and intermediate-P units, above. In the Cabo Ortegal Complex, the HP-HT units define an
84 overturned thinned sequence of rocks that is composed, from bottom to top, of quartzo-feldspathic gneisses,
85 eclogite felsic granulites and ultramafic peridotites (Fig. 1). Regarding the age of this HP-HT event, a first
86 group of authors have proposed a single event occurring during the Devonian (~390 Ma, e.g., Ordóñez Casado
87 et al., 2001) based on geochronology of eclogites and granulites. In contrast, a second group of authors have
88 found evidence of a previous HP-HT metamorphic event at Early-Ordovician times, whereas the younger
89 metamorphic event could have been definitely not older (Fernández Suárez et al., 2002). A general
90 HP/UHP-HT event occurring not before 390–400 Ma has been proposed by Arenas et al. (2014), taking
91 account regional data from different allochthonous complexes in NW Iberia and France. Those ages imply
92 Early-Middle Devonian subduction of the HP-HT allochthonous units and eventually an accretionary process
93 probably to Laurussia (Ballèvre et al., 2014; Martínez Catalán et al., 2019). This event would be interpreted as
94 the first collisional evidence of the Variscan orogeny in Europe.

95 3 Sample preparation and zircon description

96 The eclogite studied in this work is a block-in-matrix included in quartzo-feldspathic gneisses located
97 in the Cariño beach (sample COZ-4, lab number 110405, Fig. 1). The gneisses correspond to the Banded
98 Gneisses Formation defined by Vogel (1967) mainly constituted by migmatitic garnet- and kyanite-bearing
99 quartzo-feldspathic gneisses with inclusions of eclogite, mafic granulites and calc-silicate rocks (Vogel, 1967;
100 Gil Ibarguchi et al., 1990; Fernández, 1997). Lithological and mineralogical composition is heterogeneous and
101 thickness variable (> 200 m), with gradational contacts between layers locally enriched in garnet or amphibole.
102 Intercalations of leucocratic garnet-bearing orthogneisses, coronitic metagabbros and dioritic dykes evidence
103 also an old metamatism.
104 Sample COZ-4 has a granoblastic texture and it is mainly composed of omphacite and garnet with
105 honeycomb texture. Biotite, brown amphibole, calcite, sulphides and rutile appear as minor phases. The eclogite
106 block has an ellipsoid shape of ratio 1:1:2. The section YZ of the ellipsoid is a square of approximately of 1 m²
107 with sharp limits and rounded corners. It is enclosed in a phyllonite matrix formed basically by serpentinite and
108 amphibole. The matrix is well-foliated obliquely to the main foliation, whereas the eclogite block is not foliated
109 and has granoblastic texture. Oblique foliation is disposed parallel to the foliation planes of refolded decimeter-
110 scale folds and sheath folds with top-to-the-N20E sense of movement. The structural relationships between the



111 eclogite block and the banded gneisses evidence a high competence contrast, where the block is passively
112 displaced during all the deformation process.  

113 Metamorphic evolution of the enclosing eclogitic banded gneisses recorded a HP-HT event followed
114 by a fast exhumation under granulite and finally amphibolite facies metamorphism, with extensive partial
115 melting. The eclogite P-T conditions calculated from omphacite-garnet-bearing mafic rock indicated 22 kbar
116 and 780–800 °C (Basterra et al., 1989; Gil Ibarguchi et al., 1990; Mendoza, 2000; Albert et al., 2012).

117 Mineral separation was carried out at the Universidad Complutense (Madrid) and it involved an initial
118 concentration of heavy minerals using a Wilfley table, the sieving of the resulting sample below 0.2 mm, the
119 separation of the magnetic minerals with a Franz isodynamic magnetic separator, and the final concentration
120 with methylene iodide (MEI). A significant amount of heavy minerals was obtained, mainly rutile and
121 sulphides, whereas the zircon yield was poor (hardly 50 grains out of 30 kg of sample). Zircon grains are usually
122 fragments, typical of populations extracted from mafic rocks (Corfu et al., 2003), varying in size from 0.1 to 0.2
123 mm across. Still, in a few grains it is possible to recognize some crystal faces. Zircon is colorless with scarce
124 mineral or fluid inclusions.

125 The zircon grains were mounted on glass slides with a double-sided adhesive in parallel rows together
126 with some grains of zircon standard R33 (Black et al., 2004) and set in epoxy resin. After the resin was cured,
127 the mounts were ground down to expose their central portions. Prior to isotopic analysis, zircons were imaged
128 with transmitted and reflected light on a petrographic microscope, and with cathodoluminescence (CL) on a
129 JEOL 5600LV scanning electron microscope, housed at the Stanford-US Geological Survey microanalysis
130 center (SUMAC). Following the analysis, secondary electron images were taken to determine the location of the
131 spots. 

132 Cathodoluminescence images of zircon grains from sample COZ-4 display a variety of textures (Fig.
133 2). The most common CL texture is a combination of oscillatory and sector zoning (grains #5, 6, 11, 13, 14, and
134 15, Fig. 2). Some zircon grains only have a well-defined oscillatory zoning with moderate to poor luminescence
135 (grains #2, 8 and 9, Fig. 2), whereas other zircon grains exclusively show sector and fir-tree zoning with
136 moderate luminescence (grains #1, 4, 7, 10 and 16, Fig. 2). Grain #2 also displays a non-luminescent
137 homogeneous rim. There is a luminescent surrounded core (grain #3), which shows textures typically attributed
138 to metamorphism, such as recrystallization and microveining, and it is mantled by zircon with a faint soccer-ball
139 zoning, similar to grain #12. Grain #17 shows an irregular domainal texture (comparable to Fig. 3.5 in Corfu et
140 al., 2003), interpreted as a result of strain during zircon growth. This internal patchy area is partially surrounded
141 by new zircon not affected by strain and it presents broad and faint oscillatory zones.

142 In summary, following the most accepted interpretation of zircon textures (Corfu et al., 2003), most of
143 the grains exhibit zoning typical of zircon grown in an igneous environment, except grains #3, #12, #17 and the
144 rim in #2, which textures can be unequivocally interpreted as generated under metamorphic conditions.

145 **4 Results** 

146 **4.1 U-Pb SHRIMP-RG analyses** 



147 Zircon U-Th-Pb analyses were conducted on the sensitive high-resolution ion microprobe-reverse geometry
148 (SHRIMP-RG) operated by the SUMAC facility (Stanford-USGS micro analysis center) at the Stanford
149 University. An O²⁻ primary ion beam varying from 4 to 6 nA generates secondary ions from the target spot with
150 a diameter of ~20 µm and a depth of 1-2 µm. As we assumed a Paleozoic age, the counting time for ²⁰⁶Pb is
151 increased to improve counting statistics and precision of the ²⁰⁶Pb/²³⁸U age. Concentration data were normalized
152 against zircon standard CZ3 (550 ppm U, Pidgeon et al., 1994), and isotope ratios were calibrated against R33
153 (419 Ma, Black et al., 2004). Data reduction followed the methods described by Williams (1997), Ireland and
154 Williams (2003), and Squid and Isoplot 3.0 software (Ludwig, 2001, 2003) were used. The U-Pb zircon
155 data are shown in Table DR-1.

156 Twenty analyses were performed in 17 zircon grains. The youngest result has high common Pb content
157 and it will not be further considered in the discussion of the age (analysis #3.2). The following youngest result
158 obtained from a luminescent rim in grain #2 (399 Ma) and the seventeen remaining analyses are evenly
159 distributed between 382 and 403 Ma (Fig. 3). The weighted mean obtained from eight analyses is 390.4±1.2
160 Ma, with a square of weighted deviation (MSWD) of 0.65. Finally, one analysis taken in a core yields the
161 oldest age (419 Ma) and, in spite of its high common lead, its significance will be discussed later.

162 4.2 Trace element SHRIMP-RG analyses

163 After the isotopic analysis, the zircon mounts were lightly polished to remove the original gold coating
164 and sputtered pits, and recoated with gold. Methods follow those presented by Mazdab (2009). A small spot
165 diameter (about 15 µm) and a less energetic O²⁻ beam (between 1 and 2 nA) permitted that the analyses were
166 conducted in a volume adjacent to that analyzed for isotopic compositions. The primary standard MAD is a gem
167 quality crystal from Madagascar that has been extensively characterized in-house and found to be very
168 chemically homogeneous (Mazdab and Wooden, 2006). The secondary zircon standard is CZ3 (see previous
169 section). These standards were analyzed every ten unknowns over multiple analytical sessions to establish
170 precision of the trace element analyses. The procedure to obtain concentrations from raw counts is described in
171 Schwartz et al. (2010). Precision for Y at 2σ is ±6%; for the measured rare earth elements (REE, excluding La),
172 Hf, Th, and U, 2σ precision ranges from ±8 to 18%; the precision for La is ±30%.

173 Even though we performed thirty-six trace element (TE) analyses in 19 zircon grains, in this work we
174 are only reporting those analyses adjacent to a U-Pb spot (Table DR-2).

175 Uranium concentrations range from 55 to 1,150 ppm, most of the values are below 230 ppm and a
176 group of five analyses aimed to the less luminescent areas yield values higher than 370 ppm. Thorium
177 concentrations are generally low, scattered between 10 and 55 ppm, excepting the analyses in the less
178 luminescent zones, which vary between 90 and 290 ppm. In the Th-U graph (Fig. 4a), the data show a good
179 positive correlation and, with the exception of analysis #8.1, Th/U ratios are higher than 0.1.

180 Total REE concentrations are low and range from 30 to 350 ppm. In a chondrite-normalized REE
181 diagram (Fig. 4b), all analyses depict similar patterns that are characterized by a moderate fractionation from
182 lanthanum (La) to lutetium (Lu), with a prominent positive anomaly in cerium (Ce), absence of europium (Eu)



183 anomaly and a slightly negative slope in heavy (H) REE. The lack of a Eu anomaly is typically explained as the
184 result of absence of plagioclase (Rubatto, 2002), whereas the high distribution coefficient for the HREE in
185 garnet accounts for the remarkably depleted content in these elements and the resulting humped patterns in
186 zircon (Kelly and Harley, 2005, and references therein). The combination of plagioclase absence and garnet
187 presence is commonly attributed to eclogitic metamorphism (Puga et al., 2005; McClelland et al., 2006; Chen et
188 al., 2010).



189 5 Interpretation and discussion



190 5.1 Interpretation of the results

191 Even though CL images are fundamental to select the best spots for analysis in complex zircon grains, it is clear
192 that the evaluation of the geochronological results based only in the CL textures is not straightforward. In the
193 zircon grains included in this study, both CL textures and Th/U ratios strongly suggest that the obtained Middle
194 Devonian age should correspond to the igneous lith. However, this interpretation is inconsistent with
195 previous geochronology studies and with the regional geology. On one hand, the age of other mafic and felsic
196 rocks in the Iberian massif in NW Iberia varies between 470 and 470 Ma and there is no evidence of
197 a Devonian magmatic event so far (e.g., Ordóñez Casado et al., 2001; Abati et al., 2007; Fernández Suárez et
198 al., 2007; Andonaegui et al., 2012). On the other hand, several studies have suggested that there is a high-
199 pressure-high-temperature metamorphic event in this unit during the Middle Devonian (Ordóñez Casado et al.,
200 2001; Fernández Suárez et al., 2007).
201 The fallibility of the CL-Th/U-based geochronology can be easily circumvented in this case studying the REE
202 composition of zircon. Under eclogitic conditions, this mineral exhibits a couple of diagnostic features such as
203 depletion in HREE and absence of an Eu negative anomaly.



204 5.2 Origin of zircon

205 There are three main ways to form zircon in metamorphic environments (e.g., Young and Kylander-Clark,
206 2015): dissolution of existing grains and subsequent precipitation, recrystallization of former crystals, and new
207 growth, either by Zr-releasing reactions or by direct crystallization from a partial melt or a fluid.
208 Dissolution and precipitation can be used to explain the texture and isotopic data from the only grain with a
209 core-rim feature (grain #3 Fig. 2, Table DR-1). In spite of its high common Pb content, the age obtained in the
210 core (~474 Ma) is equivalent to other ages found in the literature for the eclogitic protoliths (Bernard Griffiths et
211 al., 1985; Peucat et al., 1990; Ordóñez Casado et al., 2001), whereas the rim age (~360 Ma) is probably affected
212 by lead loss. In any case, the absence of xenocrystic cores in the rest of the grains suggests that dissolution and
213 precipitation was subordinate and other zircon-forming processes were active in this eclogite.



214 Even though zircon recrystallization during metamorphism usually disturbs the former igneous zoning,
215 Schaltegger et al. (1999) report a U-loss process during zircon recrystallization that results in a weakening of
216 CL intensity, without losing the oscillatory  zoning. However, this annealing is usually coupled with partial U-Pb
217 resetting. In our case  data are tightly grouped and they are equivalent to  other ages obtained for the HP-HT
218 metamorphism in  different areas (e.g., Ordoñez Casado et al., 2001), making this argument unsound.
219 Other possibility is that new zircon grew during eclogite metamorphism. Direct crystallization from a melt or a
220 fluid has been invoked in the few studies where oscillatory zoning was found in eclogitic zircon  (Bauer et al.,
221 1997; Rubatto et al., 1998). However, crystallization from a fluid can be discarded as  zircons grown that way
222 usually have Th/U ratios lower than 0.1 (Rubatto et al., 1998). On the other hand, zircon crystallization from a
223 melt generated during eclogitic metamorphism could show Th/U ratios higher than 0.1. In that case, the system
224 would be open, making HREE available for both garnet and zircon (Rubatto, 2002). Nevertheless, the REE
225 pattern of the zircon analyzed precludes this possibility. Alternatively, zircons could be generated from
226 metamorphic reaction in solid state. The abundance of rutile suggests that titanite or ilmenite were also present
227 in the protolith, making any of these two minerals the ideal precursors for zircon (Bingen et al., 2001; Bea et al.,
228 2006).



229 5.3 Implications for the geochronology of the upper allochthon



230 The assortment of geochronological results in the upper allochthon (Fig. 5) could be  indicating that the rocks
231 grouped under this denomination have different origins, even though they are considered as different crustal
232 sections of a volcanic arc. This is coherent with the heterogeneity of the allochthonous sequences at different
233 scales, including significant differences in the structural and metamorphic evolution (e.g., Castañeiras, 2005;
234 Gómez Barreiro et al., 2006, 2007; Paquette et al., 2017). The good correlation of Lower, Middle and Upper
235 allochthon across the allochthonous complexes of NW Iberia and France support the general tectonic setting but
236 does not exclude the possibility that several lithospheric fragments were amalgamated under similar conditions
237 during the activity of the system. In addition, it should be noted that the variety of techniques and the
238 interpretation of age data does not show the  degree of robustness and could also contribute to the apparent
239 dispersion of ages (see Paquette et al., 2017; Lotout et al., 2018).

240 The combination of the trace elements (TE) signal  and a high-resolution ion probe emerges as an
241 excellent approach  to overcome regional uncertainty in the studied case as previously stated in similar context
242 (e.g. Lotout et al., 2018). The positive correlation of TE evolution and metamorphic assemblage let us connect
243 textural information and regional  evidence with geochronology, which was not considered in previous works.
244 Due to the correlation between metamorphic evolution and TE data, we suggest that the analyzed  zircons
245 represent part of the eclogites as  evidence, so that a HP event about 390 Ma is favored. It should be noted
246 that the existence of a previous (pre-400 Ma) HP event is not dismissed but specific experiments need to be
247 conducted to figure out its geological meaning (e.g. Lotout et al 2018).



248 **5.4 concluding remarks**



249 We have dated zircons from an eclogitic block-in-matrix with a combination of high-res^{ution} ion probe, CL-
250 image and TE data. Strengths and weaknesses of those techniques have been discussed and correlated with
251 regional knowledge. An age about 390 Ma has been identified and linked to an eclogite facies mineral
252 as^{age} based on zircon TE data. These data represent the most robust evidence of an eclogite facies event
253 at 390 Ma for the allochthonous complexes of the NW Iberia.

254 Our results indicate that well-known techniques (CL) and geochemical relationships (Th/U) must be used in
255 combination with TE data and structural relationships as provenance/process gauges, particularly in complex
256 orogenic scenarios or extreme environments. While geochronology provides accurate isotope relationships, their
257 temporal dimension must rely on structural and petrological evidence.

258

259 *Data availability*

260 The data are not publicly accessible

261

262 *Supplement*

263 Tables DR-1, with U-Pb isotopic zircon data, and DR-2, with REE zircon composition, is available online
264 at [\[link to be included by Solid Earth\]](#)

265

266 *Author contributions*

267 PC, JGB contributed equally to the field, experimental and elaboration of the manuscript. CA and JMBP
268 contribute to U-Pb data acquisition, processing and interpretation, and FJF participated in the fieldwork and the
269 geological interpretation.

270

271 *Competing interests*

272 The authors declare that they have no conflict of interest.

273 **Acknowledgements**

274 Carmen Valdehita is thanked for her assistance during mineral separation. Fieldwork, sample separation and
275 analytical expenses were financed by Universidad Complutense (Madrid) through the Grupo de Investigación
276 UCM Eurovarisco (910129). PC and JGB benefited from two travel aids of the “Programa de ayudas a
277 investigadores del CSIC para la realización de estancias en centros de investigación extranjeros”. CA travel was
278 financed by projects CGL-2007-66857CO2-02 and CGL2010-21298 of the Spanish Commission for Science
279 and Technology. JGB acknowledges financial support from the Ramón y Cajal Program (RYC-2010-05818).
280 Funds from the Projects CGL2010-14890 and CGL2011-23628/BTE of the Spanish Secretary of State for
281 Research, Development and Innovation and projects CGL2011-22728 and CGL2016-78560-P of the Spanish
282 Ministry of Economy, Industry and Competitiveness, as part of the National Program of Projects in
283 Fundamental Research are kindly acknowledged. JMBP appreciates financial support by the Spanish Ministry
284 of Economy, Industry and Competitiveness through the Formación de Profesional Investigador grant FPI 2013-



285 2016 (BES-2012-059893). JGB appreciates financial support by the Spanish Ministry of Science and Innovation
286 through the IEDI-2016-00691 fellowship.
287

288 **References**

- 289 Abati, J., Castiñeiras, P., Arenas, R., Fernández Suárez, J., Gómez-Barreiro, J., and Wooden, J., 2007,
290 Using SHRIMP zircon dating to unravel tectonothermal events in arc environments. The early
291 Palaeozoic arc of NW Iberia revisited, *Terra Nova*, 19, 432–439. <https://doi.org/10.1111/j.1365-3121.2007.00768.x>
- 293 Abati, J., Dunning, G.R., Arenas, R., Díaz García, F., González Cuadra, P., Martínez Catalán, J.R.,
294 and Andonaegui, P., 1999, Early Ordovician orogenic event in Galicia (NW Spain): evidence from U-
295 Pb ages in the uppermost unit of the Ordenes Complex, *Earth Planet. Sci. Lett.*, 165, 213–228.
296 [https://doi.org/10.1016/S0012-821X\(98\)00268-4](https://doi.org/10.1016/S0012-821X(98)00268-4)
- 297 Abati, J., Gerdes, A., Fernández-Suárez, J., Arenas, R., Whitehouse, M.J., and Díez-Fernández, R.,
298 2010, Magmatism and early-Variscan continental subduction in the northern Gondwana margin
299 recorded in zircons from the basal units of Galicia, NW Spain, *Geol. Soc. Am. Bull.*, 122, 219–235.
300 doi: 10.1130/B26572.1.
- 301 Albert, R., Arenas, R., Sánchez Martínez, S., and Gerdes, A., 2012, The eclogite facies gneisses of the
302 Cabo Ortegal Complex (NW Iberian Massif): Tectonothermal evolution and exhumation model, *J.
303 Iberian Geol.*, 38, 389–406, doi: 10.5209/rev_JIGE.2012.v38.n2.40465.
- 304 Anders, E., and Grevesse, N., 1989, Abundances of the elements: Meteoritic and solar, *Geochimica et
305 Cosmochimica Acta*, 53, 197–214. [https://doi.org/10.1016/0016-7037\(89\)90286-X](https://doi.org/10.1016/0016-7037(89)90286-X)
- 306 Andonaegui, P., Castiñeiras, P., González Cuadra, P., Arenas, R., Sánchez Martínez, S., Abati, J.,
307 Díaz García, F., and Martínez Catalán, J.R., 2012, The Corredoiras orthogneiss (NW Iberian Massif):
308 Geochemistry and geochronology of the Paleozoic magmatic suite developed in a peri-Gondwanan
309 arc, *Lithos*, 128–131, 84–99, doi: 10.1016/j.lithos.2011.11.005.
- 310 Arenas, R., Fernández, R.D., Martínez, S.S., Gerdes, A., Fernández-Suárez, J., Albert, R. 2014, Two-
311 stage collision: Exploring the birth of Pangea in the Variscan terranes, *Gondwana Research*, 25, 756–
312 763, doi: 10.1016/j.gr.2013.08.009.
- 313 Ayers, J.C., DeLaCruz, K., Miller, C., and Switzer, O., 2003, Experimental study of zircon coarsening
314 in quartzite ±H₂O at 1.0 GPa and 1000 °C, with implications for geochronological studies of high-
315 grade metamorphism, *American Mineralogist*, 88, 365–376. <https://doi.org/10.2138/am-2003-2-313>.
- 316
- 317 Ballèvre, M., Martínez Catalán, J.R., López-Carmona, A., Abati, J., Díez Fernández, R., Ducassou,
318 C., Pitra, P., Arenas, R., Bosse, V., Castiñeiras, P., Fernández-Suárez, J., Gómez Barreiro, J.,
319 Paquette, J.L., Peucat, J.J., Poujol, M., Ruffet, G., and Sánchez Martínez, S., 2014, Correlation of the



- 320 nappe stack in the Ibero-Armorian arc across the Bay of Biscay: a joint French-Spanish project, in
321 Schulmann, K., Oggiano, G., Lardeaux, J.M., Janousek, V., Martínez Catalán, J.R., Scrivener, R.,
322 eds., The variscan orogeny: extent, timescale and the formation of the European Crust: London,
323 Geological Society, London, Special Publications, 405, 77-113, <https://doi.org/10.1144/SP405.13>.
- 324 Basterra, R., Cassi, J.M., Pérez San Román, L., Tascon, A., and Gil Ibarguchi, J.I., 1989, Evolución
325 metamórfica de las rocas pelíticas y semipelíticas de las formaciones Banded Gneises y Gneises de
326 Cariño (Cabo Ortegal, NW España), *Studia Geologica Salmanticensia*, 4, 133–146.
- 327 Bea, F., Montero, P., and Ortega, M., 2006, A LA-ICPMS evaluation of Zr reservoirs in common
328 crustal rocks: Implications for zircon-forming processes, *Canadian Mineralogist*, 44, 745–766.
329 <https://doi.org/10.2113/gscanmin.44.3.693>
- 330 Berger, J., Féminas, O., Ohnenstetter, D., Bruguier, O., Plissart, G., Mercier, J.C.C., and Demaiffe,
331 D., 2010, New occurrence of UHP eclogites in Limousin (French Massif Central): Age, tectonic
332 setting and fluid–rock interactions, *Lithos*, 118, 365–382, doi:10.1016/j.lithos.2010.05.013.
- 333 Bernard-Griffiths, J., Peucat, J.J., Cornichet, J., Iglesias Ponce de León, M., and Gil Ibarguchi, J.I.,
334 1985, U-Pb, Nd isotope and REE geochemistry in eclogites from the Cabo Ortegal Complex, Galicia,
335 Spain: an example of REE immobility conserving MORB-like patterns during high-grade
336 metamorphism, *Chem. Geol.*, 52, 217–225. [https://doi.org/10.1016/0168-9622\(85\)90019-3](https://doi.org/10.1016/0168-9622(85)90019-3).
- 337 Bingen, B., Davis, W.J., and Austrheim, H., 2001, Zircon U-Pb geochronology in the Bergen arc
338 eclogites and their Proterozoic protoliths, and implications for the pre-Scandian evolution of the
339 Caledonides in western Norway, *Geological Society of America Bulletin*, 113, 640–649.
340 [https://doi.org/10.1130/0016-7606\(2001\)113<0640:ZUPGIT>2.0.CO;2](https://doi.org/10.1130/0016-7606(2001)113<0640:ZUPGIT>2.0.CO;2)
- 341 Black, L.P., Kamo, S.L., Allen, C.M., Davis, D.W., Aleinikoff, J.N., Valley, J.W., Mundil, R.,
342 Campbell, I.H., Korsch, R.J., Williams, I.S., and Foudoulis, C., 2004, Improved 206Pb/238U
343 microprobe geochronology by the monitoring of a trace-element-related matrix effect, SHRIMP, ID-
344 TIMS, ELA-ICP-MS and oxygen isotope documentation for a series of zircon standards, *Chemical
345 Geology*, 205, 115–140. <https://doi.org/10.1016/j.chemgeo.2004.01.003>.
- 346 Castiñeiras, P., 2005, Origen y evolución tectonotermal de las Unidades de O Pino y Cariño
347 (Complejos Alóctonos de Galicia): A Coruña, Nova Terra 28, 279 p.
- 348 Castiñeiras, P., Díaz García, F., and Gómez Barreiro, J., 2010, REE-assisted U-Pb zircon age
349 (SHRIMP) of an anatetic granodiorite: constraints on the evolution of the A Silva granodiorite,
350 Iberian Allochthonous Complexes, *Lithos*, 116, 153–166, doi: 10.1016/j.lithos.2010.01.013.
- 351 Chen Ren Xu, Zheng Yong-Fei, and Xie, Liewen, 2010, Metamorphic growth and recrystallization of
352 zircon: Distinction by simultaneous in-situ analyses of trace elements, U-Th-Pb and Lu-Hf isotopes in



- 353 zircons from eclogite-facies rocks in the Sulu orogen, *Lithos*, 114, 132–154.
354 <https://doi.org/10.1016/j.lithos.2009.08.006>.
- 355 Corfu, F., Hanchar, J.M., Hoskin, P.W.O., and Kinny, P., 2003, Atlas of zircon textures, in Hanchar,
356 J.M., and Hoskin, P.W.O., eds., *Zircon*: Washington, Mineralogical Society of America, Reviews in
357 Mineralogy and Geochemistry 53, 468–500. <https://doi.org/10.2113/0530469>.
- 358 Corfu, F., Krogh Ravna, E., and Kullerud, K., 2002, A Late Ordovician U-Pb age for HP
359 metamorphism of the Tromsdalstind eclogite of the Uppermost Allochthon of the Scandinavian
360 Caledonides: Davos, Switzerland, 12th Goldschmidt Conference, p. 18–23.
- 361
- 362 Dallmeyer, R.D., and Tucker, R.D., 1993, U-Pb zircon age for the Lagoa augen gneiss, Morais
363 Complex, Portugal: tectonic implications, *Journal of the Geological Society, London*, 150, 405–410.
364 <https://doi.org/10.1144/gsjgs.150.2.0405>
- 365 Dallmeyer, R.D., Martínez Catalán, J.R., Arenas, R., Gil Ibarguchi, J.I., Gutiérrez Alonso, G., Farias,
366 P., Aller, J., and Bastida, F., 1997, Diachronous Variscan tectonothermal activity in the NW Iberian
367 Massif: Evidence from $^{40}\text{Ar}/^{39}\text{Ar}$ dating of regional fabrics, *Tectonophysics*, 277, 307–337.
368 [https://doi.org/10.1016/S0040-1951\(97\)00035-8](https://doi.org/10.1016/S0040-1951(97)00035-8).
- 369 Díez Fernandez, R., Castiñeiras, P., and Gómez Barreiro, J., 2012a, Age constraints on Lower
370 Paleozoic convection system: magmatic events in the NW Iberian Gondwana margin, *Gondwana
371 Research*, 21, 1066–1079. <https://doi.org/10.1016/j.gr.2011.07.028>.
- 372 Díez Fernández, R., Martínez Catalán, J.R., Arenas, R., Abati, J., Gerdes, A., and Fernández Suárez,
373 J., 2012b, U-Pb detrital zircon analysis of the lower allochthon of NW Iberia: age constraints,
374 provenance and links with the Variscan mobile belt and Gondwanan cratons, *Journal of the
375 Geological Society of London*, 169, 655–665. <https://doi.org/10.1144/jgs2011-146>.
- 376 Fernández, F.J., 1997. Estructuras desarrolladas en gneises bajo condiciones de alta P y T (Gneises de
377 Chímparra, Cabo Ortegal): A Coruña, Nova Terra 13, p. 250.
- 378 Fernández-Suárez, J., Arenas, R., Abati, J., Martínez Catalán, J.R., Whitehouse, M.J., and Jeffries,
379 T.E., 2007, U-Pb chronometry of polymetamorphic high-pressure granulites: An example from the
380 allochthonous terranes of the NW Iberian Variscan belt, in Hatcher, R.D., Jr., Carlson, M.P.,
381 McBride, J.H., and Martínez Catalán, J.R., eds., *4-D Framework of Continental Crust*: Boulder,
382 Colorado, Geological Society of America Memoir 200, p. 469–488, doi: 10.1130/2007.1200(24).
- 383 Fernández-Suárez, J., Corfu, F., Arenas, R., Marcos, A., Martínez Catalán, J., García, F., Abati, J.,
384 and Fernández, F.J., 2002, U-Pb evidence for a polyorogenic evolution of the HP-HT units of the NW
385 Iberian Massif, *Contributions to Mineralogy and Petrology*, 143, 236–253.
386 <https://doi.org/10.1007/s00410-001-0337-2>.



- 387 Gebauer, D., Schertl, H., Brix, M., and Schreyer, W., 1997, 35 Ma old ultrahigh-pressure
388 metamorphism and evidence for very rapid exhumation in the Dora Maira Massif, Western Alps,
389 *Lithos*, 41, 5–24. [https://doi.org/10.1016/S0024-4937\(97\)82002-6](https://doi.org/10.1016/S0024-4937(97)82002-6).
- 390 Gil Ibarguchi, J.I., Mendoza, M., Girardeau, J., and Peucat, J.J., 1990, Petrology of eclogites and
391 clinopyroxene-garnet metabasites from the Cabo Ortegal Complex (northwestern Spain), *Lithos*, 25,
392 133–162, [https://doi.org/10.1016/0024-4937\(90\)90011-O](https://doi.org/10.1016/0024-4937(90)90011-O).
- 393 Gómez Barreiro, J., Martínez Catalán, J.R., Arenas, R., Castañeiras, P., Abati, J., Díaz García, F., and
394 Wijbrans, J.R., 2007, Tectonic evolution of the upper allochthon of the Órdenes Complex
395 (northwestern Iberian Massif): structural constraints to a polyorogenic peri-Gondwanan terrane, *in*
396 Linnemann, U., Nance, R.D., Kraft, P., and Zulauf, G., eds., *The evolution of the Rheic Ocean: from*
397 *Avalonian–Cadomian active margin to Alleghenian–Variscan collision: Boulder, Colorado,*
398 Geological Society of America Special Paper 423, 315–332. [https://doi.org/10.1130/2007.2423\(15\)](https://doi.org/10.1130/2007.2423(15)).
- 399 Gómez Barreiro, J., Wijbrans, J.R., Castañeiras, P., Martínez Catalán, J.R., Arenas, R., Díaz García, F.,
400 and Abati, J., 2006, 40Ar/39Ar laser probe dating of mylonitic fabrics in polyorogenic terrane of NW
401 Iberia, *Journal of the Geological Society of London*, 163, 61–73. <https://doi.org/10.1144/0016-7649-05-012>
- 403 Harley S.L., and Black L.P., 1997, A revised Archaean chronology for the Napier Complex, Enderby
404 Land, from SHRIMP ion-microprobe studies, *Antarctic Science*, 9, 74–91.
405 <https://doi.org/10.1017/S0954102097000102>.
- 406 Harley, S.L., Kelly, N.M., and Möller, A., 2007, Zircon behaviour and the thermal histories of
407 mountain chains, *Elements*, 3, 25–30. <https://doi.org/10.2113/gselements.3.1.25>
- 408 Hermann, J., Rubatto, D., Korsakov, A., and Shatsky, V., 2001, Multiple zircon growth during fast
409 exhumation of diamondiferous, deeply subducted continental crust (Kokchetav Massif, Kazakhstan),
410 *Contributions to Mineralogy and Petrology*, 141, 66–82. <https://doi.org/10.1007/s004100000218>
- 411 Ireland, T.R., and Williams, I.S., 2003, Considerations in zircon geochronology by SIMS, in Hanchar,
412 J.M., and Hoskin, P.W.O., eds., *Zircon: Washington*, Mineralogical Society of America, *Reviews in*
413 *Mineralogy and Geochemistry*, 53, 215–241. <https://doi.org/10.2113/0530215>
- 414 Kelly, N.M., and Harley, S.L., 2005, An integrated microtextural and chemical approach to zircon
415 geochronology: refining the Archean history of the Napier Complex, east Antarctica, *Contributions to*
416 *Mineralogy and Petrology*, 149, 57–84. <https://doi.org/10.1007/s00410-004-0635-6>.
- 417 Korotev, R.L. 1996, A self-consistent compilation of elemental concentration data for 93 geochemical
418 reference samples, *Geostandards Newsletter*, 20, 217–245. <https://doi.org/10.1111/j.1751-908X.1996.tb00185.x>.
- 420 Kuijper, R.P., Priem, H.N.A., and Den Tex, E., 1982, Late Archaean-early proterozoic source ages of
421 zircons in rocks from the Paleozoic orogen of western Galicia, NW Spain, *Precambrian Research*, 19,
422 1–29, doi: 10.1016/0301-9268(82)90017-1.



- 423 Lati, A., and Gebauer, D., 1999, Constraining the prograde and retrograde P-T-t path of Eocene HP
424 rocks by SHRIMP dating of different zircon domains: inferred rates of heating, burial, cooling and
425 exhumation for central Rhodope, northern Greece, Contributions to Mineralogy and Petrology, 135,
426 340–354, <https://doi.org/10.1007/s004100050516>.
- 427 López Carmona, A., Pitra, P., and Abati, J., 2013, Blueschist-facies metapelites from the Malpica-Tui
428 Unit (NW Iberian Massif): phase equilibria modelling and H₂O and Fe₂O₃ influence in high-pressure
429 assemblages, Journal of Metamorphic Geology, 31, 263–280, <https://doi.org/10.1111/jmg.12018>.
- 430 Lotout, C., Pitra, P., Poujol, M., Anczkiewicz, R., and Van Den Driessche, J. (2018). Timing and
431 duration of Variscan high-pressure metamorphism in the French Massif Central: A multimethod
432 geochronological study from the Najac Massif. Lithos, 308, 381-394.
433 <https://doi.org/10.1016/j.lithos.2018.03.022>.
- 434 Ludwig, K.R., 2001, Squid, A users manual, Berkeley Geochronology Center Special Publication No.
435 2.
- 436 Ludwig, K.R., 2003, Isoplot 3.00, a geochronological toolkit for Excel, Berkeley Geochronology
437 Center Special Publication No. 4.
- 438 Martínez Catalán, J.R., Arenas, R., Abati, J., Sánchez Martínez, S., Díaz García, F., Fernández
439 Suárez, J., González Cuadra, P., Castiñeiras, P., Gómez Barreiro, J., Díez Montes, A., González
440 Clavijo, E., Rubio Pascual, F.J., Andonaegui, P., Jeffries, T.E., Alcock, J.E., Díez Fernández, R., and
441 López Carmona, A., 2009, A rootless suture and the loss of the roots of a mountain chain: The
442 Variscan belt of NW Iberia, Comptes Rendus Geoscience, 341, 114–126.
443 <https://doi.org/10.1016/j.crte.2008.11.004>.
- 444 Martínez Catalán, J.R., Gómez Barreiro, J., Dias da Silva, I., Chichorro, M., López-Carmona, A.,
445 Castiñeiras, P., Abati, J., Andonaegui, P., Fernández-Suárez, J., González Cuadra, P., Benítez-Pérez,
446 J. M. (2019): Variscan Suture Zone and Suspect Terranes in the NW Iberian Massif: Allochthonous
447 Complexes of the Galicia-Trás os Montes Zone (NW Iberia). In: Quesada, C. and Oliveira, T. (eds.):
448 *The Geology of Iberia: A Geodynamic Approach*, pp. 99-130. Springer, Cham.
449 https://doi.org/10.1007/978-3-030-10519-8_4.
- 450 Mateus, A., Munhá, J., Ribeiro, A., Tassinari, C. C. G., Sato, K., Pereira, E., and Santos, J. F. (2016).
451 U-Pb SHRIMP zircon dating of high-grade rocks from the Upper Allochthonous Terrane of Bragança
452 and Morais Massifs (NE Portugal): geodynamic consequences. Tectonophysics, 675, 23-49.
453 <https://doi.org/10.1016/j.tecto.2016.02.048>.
- 454 Mazdab, F.K., 2009, Characterization of flux-grown trace-element-doped titanite using the high-
455 mass-resolution ion microprobe (SHRIMP-RG), Canadian Mineralogist, 47, 813–831.
456 <https://doi.org/10.3749/canmin.47.4.813>.
- 457 Mazdab, F.K., and Wooden, J.L., 2006, Trace element analysis in zircon by ion microprobe
458 (SHRIMP-RG): technique and applications, Geochimica et Cosmochimica Acta Supplement, 70, 405,
459 10.1016/j.gca.2006.06.817.



- 460 McClelland, W.C., Power, S.E., Gilotti, J.A., Mazdab, F.K., and Wopenka, B., 2006, U-Pb SHRIMP
461 geochronology and trace-element geochemistry of coesite-bearing zircons, North-East Greenland
462 Caledonides, *in* Hacker, B.R., McClelland, W.C., and Liou, J.G., eds., Ultrahigh-pressure
463 metamorphism: Deep continental subduction: Boulder, Colorado. Geological Society of America
464 Special Paper 403, 23–43, [https://doi.org/10.1130/2006.2403\(02\)](https://doi.org/10.1130/2006.2403(02)).
- 465 Mendia, M.S., 2000, Petrología de la Unidad Eclogítica del Complejo de Cabo Ortegal (NW de
466 España): A Coruña, Nova Terra 16, p. 424.
- 467 Ordoñez Casado, B., Gebauer, D., Schäfer, H.J., Ibarguchi, G., and Peucat, J.J., 2001, A single
468 Devonian subduction event for the HP/HT metamorphism of Cabo Ortegal complex within the Iberian
469 Massif, Tectonophysics, 3, 359–385, [https://doi.org/10.1016/S0040-1951\(00\)00210-9](https://doi.org/10.1016/S0040-1951(00)00210-9).
- 470 Peucat, J.J., Bernard-Griffiths, J., Gil Ibarguchi, J.I., Dallmeyer, R.D., Menot, R.P., Cornichet, J., and
471 Iglesias Ponce de Leon, M., 1990, Geochemical and geochronological cross section of the deep
472 Variscan crust: The Cabo Ortegal high-pressure nappe (Northwestern Spain), Tectonophysics, 177,
473 263–292. [https://doi.org/10.1016/0040-1951\(90\)90285-G](https://doi.org/10.1016/0040-1951(90)90285-G).
- 474 Paquette, J. L., Ballèvre, M., Peucat, J. J., Cornen, G. (2017). From opening to subduction of an
475 oceanic domain constrained by LA-ICP-MS U-Pb zircon dating (Variscan belt, Southern Armorican
476 Massif, France). Lithos, 294, 418-437. <https://doi.org/10.1016/j.lithos.2017.10.005>.
- 477 Pidgeon R.T., Furfarro D., Kennedy A.K., Nemchin A.A., Van Bronswijk W., 1994, Calibration of
478 zircon standards for the Curtin SHRIMP II: Abstracts of the eighth International Conference on
479 Geochronology, Cosmochronology and Isotope Geology, U.S. Geological Survey Circular v. 1107, p.
480 251.
- 481 Puga, E., Fanning, C.M., Nieto, J.M., and Díaz de Federico A., 2005, Recrystallization textures in
482 zircon generated by ocean-floor and eclogite-facies metamorphism, a cathodoluminescence and U-Pb
483 SHRIMP study, with constraints from REE elements, Canadian Mineralogist, 43, 183–202.
484 <https://doi.org/10.2113/gscanmin.43.1.183>.
- 485
- 486 Roberts, M., and Finger, F., 1997, Do U-Pb zircon ages from granulites reflect peak metamorphic
487 conditions?, Geology, 25, 319–322. [https://doi.org/10.1130/0091-
488 7613\(1997\)025<0319:DUPZAF>2.3.CO;2](https://doi.org/10.1130/0091-7613(1997)025<0319:DUPZAF>2.3.CO;2).
- 489 Rubatto, D., 2002, Zircon trace element geochemistry: partitioning with garnet and the link between
490 U-Pb ages and metamorphism, Chemical Geology, 184, 123–138. [https://doi.org/10.1016/S0009-2541\(01\)00355-2](https://doi.org/10.1016/S0009-
491 2541(01)00355-2).
- 492 Rubatto, D., and Gebauer, D., 2000, Use of cathodoluminescence for U-Pb zircon dating by ion
493 microprobe: some examples from the Western Alps, *in* Pagel M., Barbin V., Blanc P., and
494 Ohnenstetter D., eds., Cathodoluminescence in geosciences: Berlin, Springer, 373–400.
495 https://doi.org/10.1007/978-3-662-04086-7_15.



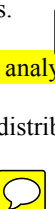
- 496 Rubatto, D., Gebauer, D., and Fanning, M., 1998, Jurassic formation and Eocene subduction of the
497 Zermatt-Saas-Fee ophiolites: Implications for the geodynamic evolution of the Central and Western
498 Alps, Contributions to Mineralogy and Petrology, 132, 269–287,
499 <https://doi.org/10.1007/s004100050421>.
- 500 Santos Zalduogui, J.F., Schärer, U., Gil Ibarguchi, J.I., and Girardeau, J., 1996, Origin and evolution
501 of the Paleozoic Cabo Ortegal ultramafic-mafic complex (NW Spain): U-Pb, Rb-Sr and Pb-Pb isotope
502 data, Chemical Geology, 129, 281–304, [https://doi.org/10.1016/0009-2541\(95\)00144-1](https://doi.org/10.1016/0009-2541(95)00144-1).
- 503 Schaltegger U., Fanning C.M., Günther D., Maurin J.C., Schulmann K., and Gebauer D., 1999,
504 Growth, annealing and recrystallization of zircon and preservation of monazite in high-grade
505 metamorphism: conventional and in-situ U-Pb isotope, cathodoluminescence and microchemical
506 evidence, Contributions to Mineralogy and Petrology, 134, 186–201.
507 <https://doi.org/10.1007/s004100050478>.
- 508 Schwartz, J.J., John, B.E., Cheadle, M.J., Wooden, J.L., Mazdab, F., Swapp, S., and Grimes, C.B.,
509 2010, Dissolution-reprecipitation of igneous zircon in mid-ocean ridge gabbro, Atlantis Bank,
510 Southwest Indian Ridge, Chemical Geology, 274, 68–81.
511 <https://doi.org/10.1016/j.chemgeo.2010.03.017>.
- 512 Tomaschek, F., Kennedy, A., Villa, I., Lagos, M., and Ballhaus, C., 2003, Zircons from Syros,
513 Cyclades, Greece-Recrystallization and mobilization of zircon during high-pressure metamorphism,
514 Journal of Petrology, 44, 1977–2002. <https://doi.org/10.1093/petrology/egg067>.
- 515 Valverde Vaquero, P., and Fernández, F.J., 1996, Edad de enfriamiento U/Pb en rutilos del Gneis de
516 Chímparra (Cabo Ortegal, NO de España), Geogaceta, v. 20, p. 475–478.
- 517 van Calsteren, P.W.C., Boelrijk, N.A.I.M., Hebeda, E.H., Priem, H.N.A., Den Tex, E., Verduren,
518 E.A.T.H., and Verschure, R.H., 1979, Isotopic dating of older elements (including the Cabo Ortegal
519 mafic-ultramafic complex) in the Hercynian orogen of NW Spain: manifestations of a presumed Early
520 Paleozoic mantle plume, Chemical Geology, 24, 35–56. [https://doi.org/10.1016/0009-2541\(79\)90011-1](https://doi.org/10.1016/0009-2541(79)90011-1).
- 522 Vavra, G., Schmid, R., and Gebauer, D., 1999, Internal morphology, habit and U-Th-Pb microanalysis
523 of amphibolite-to-granulite facies zircons: geochronology of the Ivrea Zone (Southern Alps),
524 Contributions to Mineralogy and Petrology, 134, 380–404. <https://doi.org/10.1007/s004100050492>.
- 525 Vogel, D.E., 1967, Petrology of an eclogite- and pirigarnite-bearing polymetamorphic rock complex
526 at Cabo Ortegal, NW Spain, Leidse Geologische Mededelingen, 40, 121–213.
- 527 Williams, I.S., 1997, U-Th-Pb geochronology by ion microprobe: not just ages but histories, Reviews
528 in Economic Geology, 7, 1–35. <https://doi.org/10.5382/Rev.07.01>.
- 529 Young, D.J. and Kylander-Clark, A.R.C., 2015, Does Continental Crust Transform during Eclogite-
530 Facies Metamorphism?, Journal of Metamorphic Geology, 33, 331–357.
531 <https://doi.org/10.1111/jmg.12123>.
- 532



533 **FIGURE CAPTIONS**

534 Figure 1. Geological map of the northern area of the Cabo Ortegal Complex with the location
535 of the sample. 

536 Figure 2. Cathodoluminescence images of the analyzed zircons. Ellipses indicate the location
537 of the U-Pb spots, whereas circles represent the trace element analyses. 

538 Figure 3. (A) Tera-Wasserburg diagram showing U-Pb data for the analyzed sample. Gray
539 ellipses represent data included in the calculated mean. (B) Age distribution of the data
540 considered in the mean age calculation. 

541 Figure 4. (A) U versus Th and (B) chondrite-normalized REE patterns. Normalization values
542 after Anders and Grevesse (1989), modified by Korotev (1996). 

543 Figure 5. Protolith and metamorphism ages in the upper allochthon, including the HP-HT and
544 the IP units. Abbreviations: Zrn, zircon; Mnz, monazite; Hbl, hornblende; Am, amphibole;
545 Ms, muscovite; Bt, biotite; Ttn, titanite; Ep, epidote; Rt, rutile; Phl, phlogopite; Ed, edenite;
546 WR, whole-rock; rcl, recalculated by Kuilper et al. (1982).

547

548 **Supplementary data**

549 Tables DR-1, with U-Pb isotopic zircon data, and DR-2, with REE zircon composition, is
550 available online at [\[link to be included by Solid Earth\]](#)



Figure 1

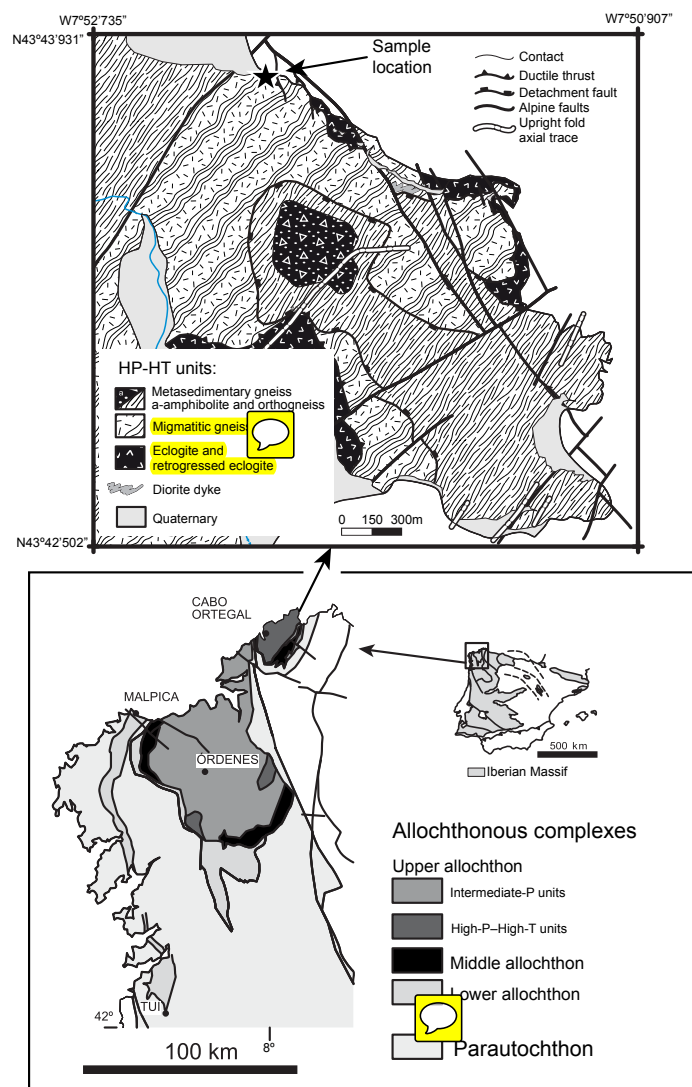




Figure 2

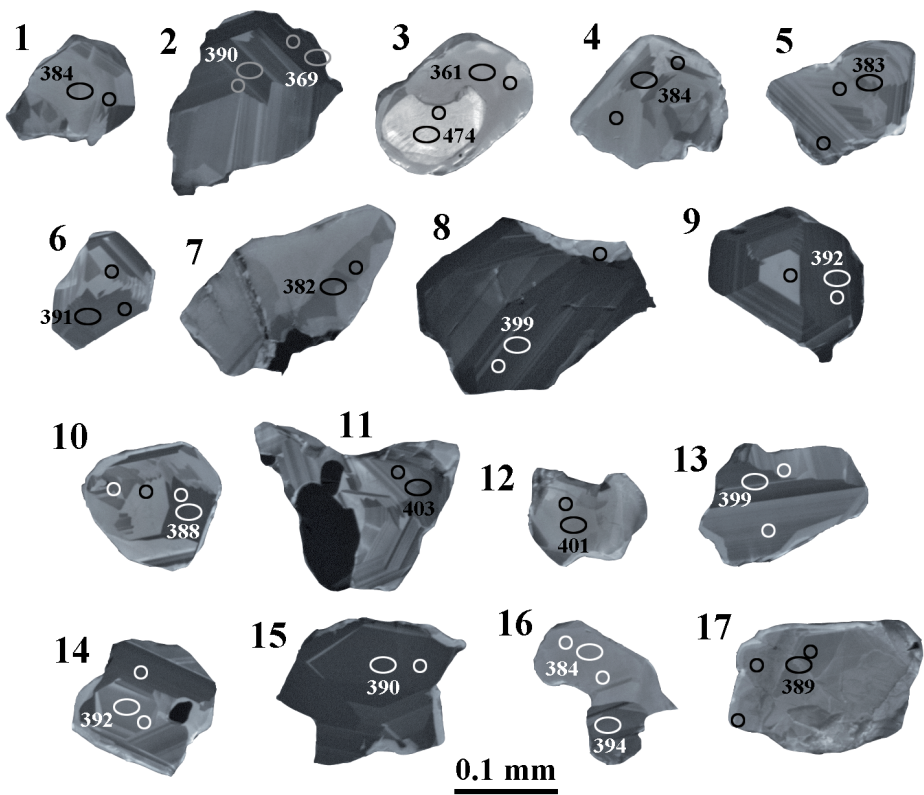




Figure 3

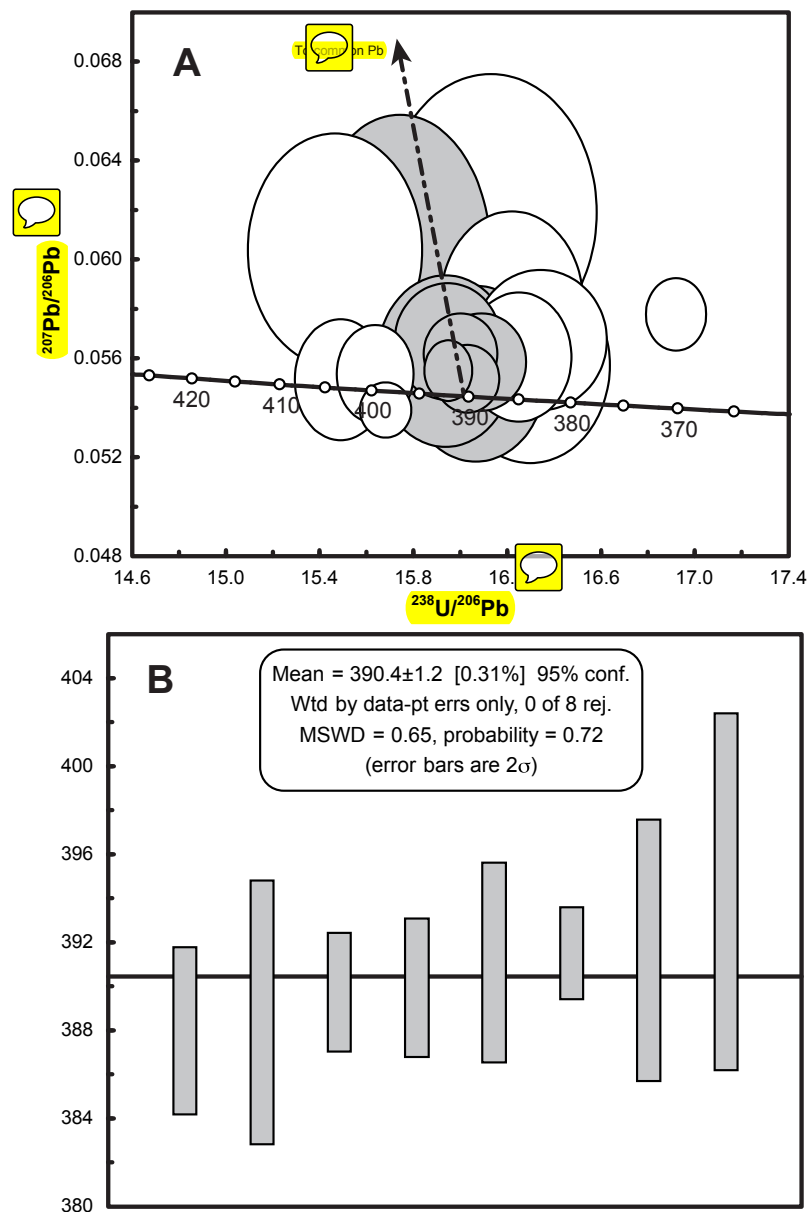




Figure 4

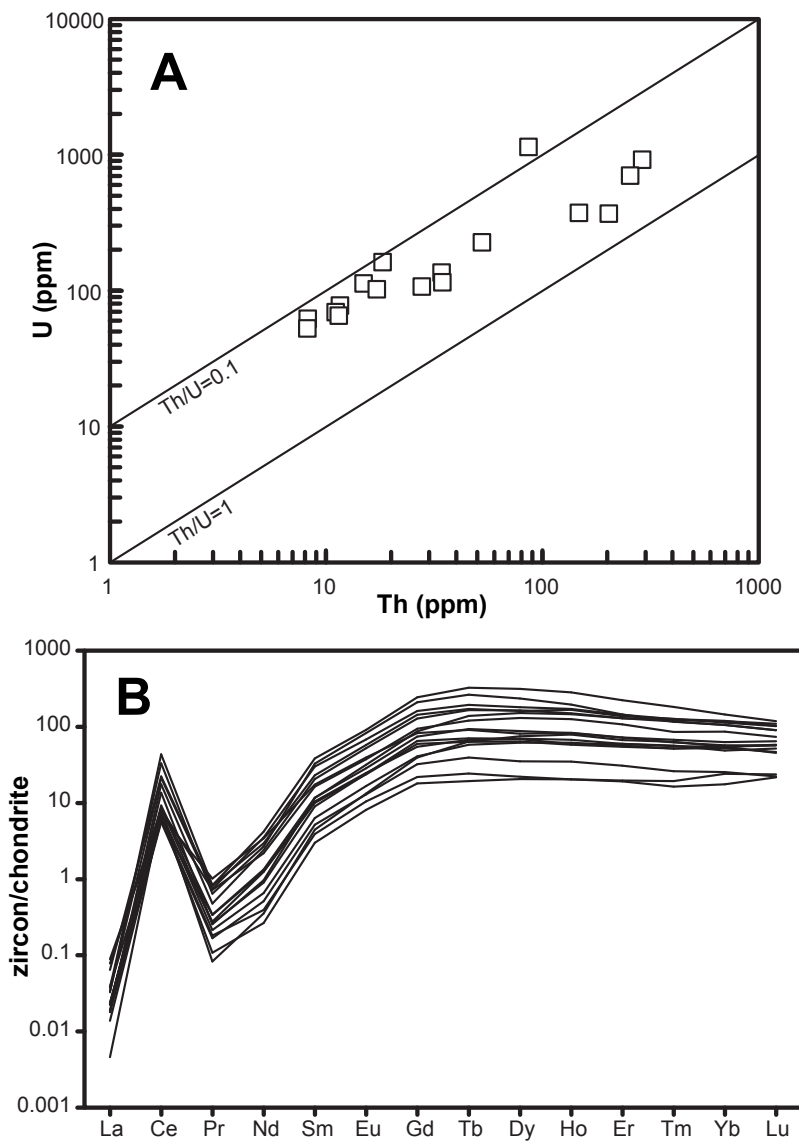




Figure 5

